Radiol med (2015) 120:228–238
DOI 10.1007/s11547-014-0431-y

MAGNETIC RESONANCE IMAGING

Transvaginal ultrasound assessment of uterine scar after previous caesarean section: comparison with 3T-magnetic resonance diffusion tensor imaging

Federica Fiocchi · Elisabetta Petrella · Luca Nocetti · Serena Currà · Guido Ligabue · Tiziana Costi · Pietro Torricelli · Fabio Facchinetti

Received: 13 July 2013 / Accepted: 28 February 2014 / Published online: 7 August 2014

Abstract

Purpose This study aimed to evaluate 3-T magnetic resonance imaging in the analysis of caesarean scars in women with prior caesarean section (pCS) and investigate the potential added value of diffusion tensor imaging (3T-MR-DTI) with fibre tracking reconstruction, compared with transvaginal ultrasound (TVUS).

Methods Thirty women who had previously undergone elective CS in a singleton pregnancy at term were examined (19 women with one pCS formed group 1 and 11 women with two pCS formed group 2). Patients underwent TVUS and 3T-MR-DTI within 2 days. Twelve women with prior vaginal delivery served as controls and underwent only 3T-MR. Uterine fibre architecture was depicted by MR-DTI with 3D tractography reconstruction providing quali-quantitative analysis of fibre, described as the reduction of number of longitudinal fibres that run through the uterine scar.

Results Six subjects were excluded. According to 3T-MR morphology, scars were described as linear ($n = 12$) and retracting ($n = 12$); disagreement with TVUS was 54 %. The thickness of myometrium at the scar level was found to be significantly greater with 3T-MR compared to TVUS in linear scars ($p = 0.01$). No difference was found among retracting scars. In controls, according to 3T-MR-DTI, longitudinal myometrial fibres running in the anterior wall were similar to those in the posterior wall at same level −2 %; −27 % + 22 %). In groups 1 and 2 there was significant reduction in anterior fibres compared to posterior ones (−53 %; −77 % − 34 %; $p = 0.0001$). Among retracting scars, fibre reduction was significantly higher compared to linear scars, $p < 0.016$.

Conclusions The added value of 3T-MR with DTI lies in the prompt evaluation of muscle fibre remaining at scar level.

Keywords 3T-MRI · Diffusion tensor imaging · Caesarean Scar · Fibre tracking

F. Fiocchi (✉) · S. Currà · G. Ligabue
Department of Radiology, University of Modena and Reggio Emilia, Via del Pozzo 71, 41124 Modena, Italy
e-mail: federica.fiocchi@gmail.it

E. Petrella · P. Torricelli · F. Facchinetti
Mother-Infant Department, University of Modena and Reggio Emilia, Via del Pozzo 71, 41124 Modena, Italy

L. Nocetti · T. Costi
Medical Physics Department, University of Modena and Reggio Emilia, Via del Pozzo 71, 41124 Modena, Italy

Introduction

The overall rate of caesarean section (CS) has dramatically increased in developed countries over the last decade [1]. This has led to an increase in abnormalities of placentation such as placenta previa and/or accreta [2–6] and uterine rupture [7–10]. The WHO Global Survey on Maternal and Perinatal Health, a large cross-sectional study conducted across 24 countries, concluded that CS is associated with an increased risk of both maternal and fetal morbidity and mortality [11]. Therefore, most guidelines advocate trial of labour after prior CS (pCS) [12, 13].

Thus, investigators have focused on finding a more precise method of scar evaluation in order to create an objective tool to predict which pregnancies are at risk following pCS. To select women with the lowest risk of uterine rupture, some authors [14–20] suggested the use of the sonographic measurement of the lower uterine segment

(LUS) thickness near term. Unfortunately, this did not become recommended clinical practise because the optimal cutoff values and measurement techniques remain controversial. Moreover, transvaginal ultrasound (TVUS) has several limitations regarding the analysis of uterine scar morphology, namely myometrial thickness, in nonpregnant women [21–26]. According to these studies, large scar defects have been found in various proportions of women who have undergone CS, and the rate of large scar defects increases with the number of caesarean deliveries [22–24].

Currently, the clinical importance of large scar defects is unknown. It is possible that they entail a greater risk of complications in subsequent pregnancies (such as uterine rupture or abnormalities in placentation) than intact scars or scars with only small defects. However, this remains an open issue.

Magnetic resonance (MR) is another imaging modality that has a well-established role in studying the female pelvis, especially at high field strengths (3 T) [27–31]. MR with diffusion tensor imaging (MR-DTI) and fibre tracking reconstruction is a novel noninvasive imaging technique that could characterise tissue morphology by measuring the amount of random diffusion (Brownian motion) of water molecules throughout the tissue [32]. As water molecules diffuse more easily along organised structures, such as muscle fibres, rather than across them, MR-DTI can highlight the muscle fibre architecture of the uterus. This method has been applied in one study on ex vivo uteri allowing the estimation of uterine muscle fibre direction or anisotropy [33]. Recently, our research group showed that this method could be used to describe the uterine muscle architecture in vivo and that women with pCS showed various degrees of disarray [34].

Therefore, the aims of the present study were as follows: to compare TVUS with 3T-MR in the morphological evaluation of caesarean scar, and to investigate the potential added value of MR-DTI with fibre tracking reconstruction in assessing uterine scars in women with pCS.

Materials and methods

Subjects

This was an observational open study. The protocol was approved by the Local Ethics Committee (protocol number 3848/10). All volunteers gave written informed consent.

Eligible subjects were women with one or two pCS who were enrolled between December 2010 and December 2012. Primiparous women with one previous vaginal delivery served as the control group.

The inclusion criteria were the following: age 18–45 years, Caucasian ethnicity, and a prior singleton gestation delivered by elective CS (with a low transverse uterine incision) without labour within 24 months. Exclusion criteria were the following: multiple gestations, more than two pCS, trial of labour after the first CS, women with uterine myomas, uterine retroversion or retroflexion, use of hormonal contraception, and women with other previous uterine scars, post-partum endometritis, pelvic inflammatory disease and tubal ligation, as well as those with generic exclusion criteria for MR.

Study design

All volunteers underwent TVUS (Esaote Mylab 50 XVision) and 3T-MR with DTI (Philips Achieva, The Best, Netherlands) within 2 days of each other. Two independent operators performed the imaging. Each operator knew which group the patient belonged to but was unaware of the result of the other examination. Women were examined during the follicular phase and a negative pregnancy test was required.

To compare TVUS to 3T-MR in the morphological assessment of caesarean scar at the hysterectomy site, the myometrial thickness was measured, by both methods, from the endometrial interface to the serosa at the following three levels: at the scar level, upstream and downstream of the scar.

All subjects underwent 3T MR-DTI with fibre tracking reconstruction for the assessment of the uterine scar, which provided supplementary quali-quantitative information about the microstructural disarray of the uterine myometrial fibres.

Methods

TVUS technique

All TVUS were performed using transvaginal 7 MHz ultrasonography (Esaote Mylab 50 X Vision). All women were examined in a supine position with an empty bladder during the follicular phase of the menstrual cycle. The uterus was examined in the longitudinal and coronal planes. First, conventional grey-scale ultrasound examination of the endometrium was performed. The analysis of grey-scale ultrasound endometrial morphology included visual evaluation of regularity of the endometrial–myometrial border and endometrial thickness. Subsequently, myometrial morphology and echogenicity were evaluated, and the myometrial thickness was measured.

3T-MR technique

All patients underwent 3T-MR imaging (Achieva, Philips Medical Systems, Best, The Netherlands) using a 6-channel

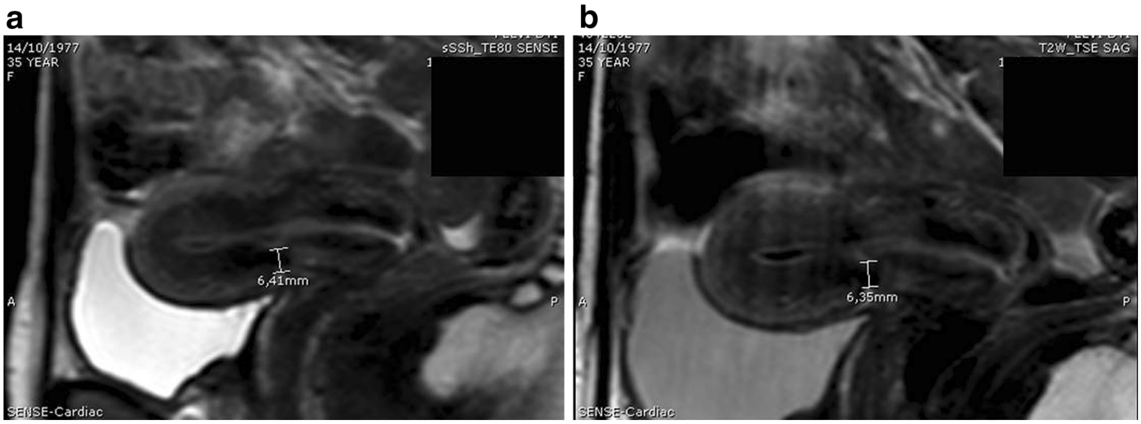

Fig. 1 35-year-old woman with one caesarean delivery and subsequent vaginal delivery. **a** Single-shot turbo spin-echo (Ssh-TSE) T2 image on the uterine proper long axis with reported measurement at scar level (scar classified as linear), **b** TSE T2 image on uterine proper long axis with reported measurement at scar level (scar classified as linear)

coil-phased array Synergy–Cardio in the supine position. The maximum gradient strength was 40 mT/m, and the maximum slew-rate was 200 $Tm^{-1}s^{-1}$. The study protocol included preliminary morphologic spin-echo (SE) sequences of the female pelvis (from the renal hila to the pubic symphysis), three fast sequences (single-shot turbo spin-echo—Ssh-TSE) on the proper long and short axes of the uterus in order to plan a diffusion-weighted sequence for the multiple directions used for DTI imaging. A parasagittal morphological TSE T2 sequence was later performed on uterus proper long axis (Fig. 1).

All volunteer subjects were asked to fast beginning at midnight to avoid significant differences in body temperature.

Sequences parameters were as follows:

- Axial T1-weighted spin echo (SE): TE 10 ms, TR 600 ms, field of view (FOV) 21 × 21 cm, matrix 256 × 256, thickness 4 mm, gap 1 mm, number of signal acquisition (NSA) 2;
- Axial, sagittal and para-sagittal T2-weighted single-shot turbo SE (Ssh-TSE): TE 80 ms, TR 1300 ms, FOV 35 × 25 × 15 cm, matrix 300 × 175, thickness 5 mm, NSA 1, Sense 2. The para-sagittal plane was acquired considering the body sagittal plane rotated on the long axis of the uterus.
- Parasagittal T2 TSE sequence: TE 80, TR > 2500, FOV 35 × 25 × 15 cm, matrix 256 × 328, thickness 3, gap 0.5, NSA 2, CLEAR yes.

A diffusion-weighted sequence is a fast echo-planar sequence (Ssh-EPI), where multiple echoes are acquired in order to minimise artefacts from movement [32]. Uterine contractions and intestinal peristalsis can create artefacts that disturb image acquisition and invalidate the results. Diffusion-weighted Ssh-EPI was acquired with spectral fat saturation and half-Fourier sampling along 16 directions to obtain tensor imaging (DTI). Sequences were obtained with $b = 600$ mm²/s.

Diffusion-weighted Ssh-EPI was performed on the parasagittal plane with the following parameters:

- TE 70 ms, TR > 5000 ms, FOV 31 × 31 × 84 cm, matrix 140 × 140, thickness 2.1 mm, NSA 2, Epi factor 135, fold-over AP, $b = 600$ mm²/s.

3T-MR image post-processing

Diffusion-weighted Ssh-EPI images were processed on a dedicated workstation for data pre-processing with MedINRIA software (MedINRIA v2.0, Medical Image Navigation and Research tool by Sophia Antipolis, Research project ASCLEPIOS). Diffusion eigenvalues and eigenvectors were estimated in each voxel in order to calculate fractional anisotropy and the apparent diffusion coefficient map; then, through a proper visualisation tool (Deterministic DTI Track; MedINRIA 2.0), fibre tracking is performed. Tracking was continued until the chosen criteria were met (for example, minimal fractional anisotropy (FA) of 0.2 and a maximal angle change of 10° per integration step). Fibres underlining the preferential water movement used a reference vector colour-coded map (assigning red, green and blue to each orthogonal direction). Within 5–10 min, all fibres were appreciable, but if fibres of all the voxels that constitute the uterus were used in this fashion, it resulted in no visible structures. The dimension and the location of the different regions of interest (ROI) were drawn on the basis of what we wanted to visualise, and thus to obtain simple to complex structures following different interpretations. Therefore, a reduction of fibres was applied to reveal at first the global uterine architecture and then the

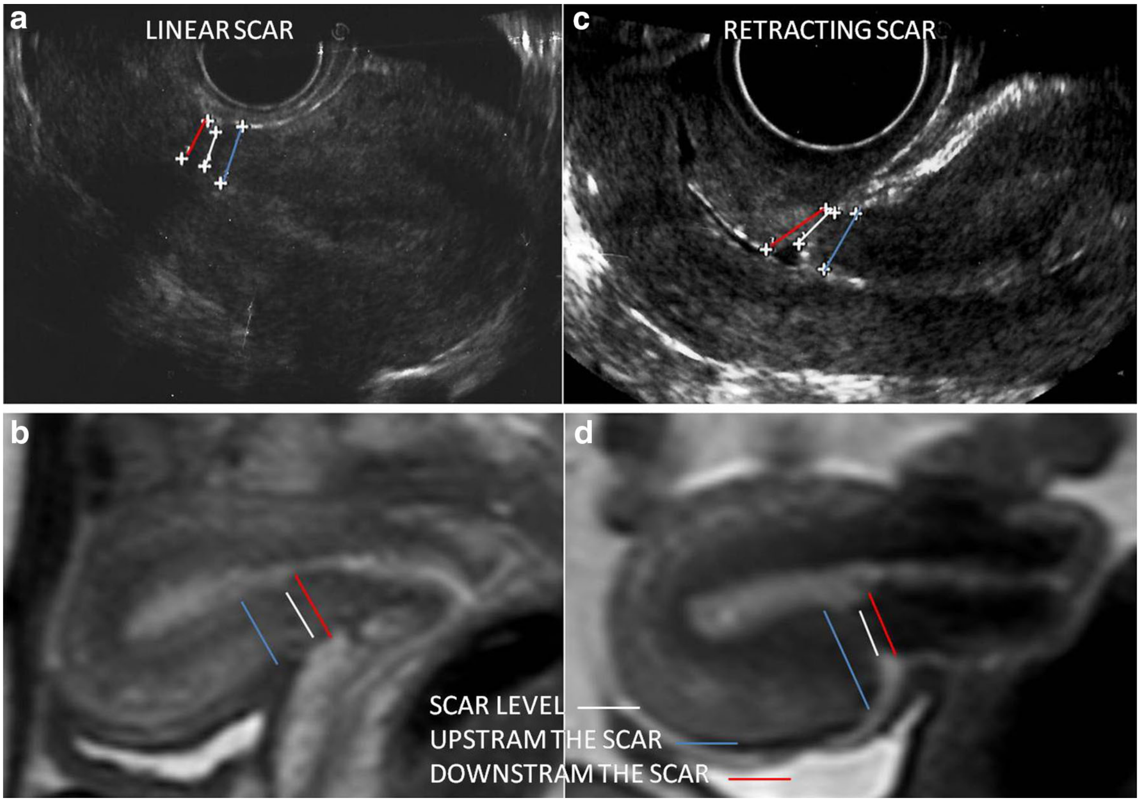

Fig. 2 Morphological subjective description of the caesarean scar; comparison between transvaginal ultrasound (TVUS) and magnetic resonance imaging at 3 Tesla (3T-MR); myometrial thickness evaluation over the scar, *upstream* and *downstream* of the scar. **a, b** "*Linear scar*" measurements by TVUS and 3T-MR, respectively. **c, d** "retracting scar" measurements by TVUS and 3T-MR, respectively

specific orientation and distribution of the fibres. To identify longitudinal or circular fibres, different ROI were placed on the uterus, particularly on the isthmus.

The feasibility of the techniques described above has been validated in a previous study on nulliparous volunteers and volunteers with previous vaginal or caesarean deliveries [34].

Image analysis

Scars were subjectively classified by TVUS and 3T-MR as follows:

1. linear, if the endometrial profile was not altered;
2. retracting, if the endometrial profile was altered or the myometrium was thinned, or in the presence of endometrial dehiscence. At the level of the scar, thinning and retraction of the anterior myometrium frequently create wedge-shaped defects on both the serosal and endometrial sides. This distortion and prominence of the tissues adjacent to the scar often have an hourglass shape on sagittal views [30].

Endometrial thickness was measured in both modalities in a median longitudinal plane of the uterus as the maximum distance between the endometrial–myometrial interface of the anterior to the posterior wall of the uterus [29].

Myometrial thickness was measured from endometrial interface to serosa at the following three levels: at the scar level (myometrium over the defect), upstream of the scar (the thickness of the myometrium close to and fundal to the defect) and downstream of the scar (the thickness of the myometrium close to the inner cervical ostium) (Fig. 2). All these measurements were obtained with TVUS and 3T-MR.

Furthermore, uterine fibre architecture was depicted with MR-DTI with a 3D tractography reconstruction (Fig. 3). After a qualitative reconstruction of fibre orientation, a quantitative analysis of the number of longitudinal fibres that ran through uterine scar (on the anterior isthmus) was performed comparing the fibres running in the posterior wall at the same level.

These quantitative data were compared with the number of CS and the time elapsed between CS.

Statistical analysis

Statistical analysis was performed using both parametric and nonparametric tests, as required. Within- and between-

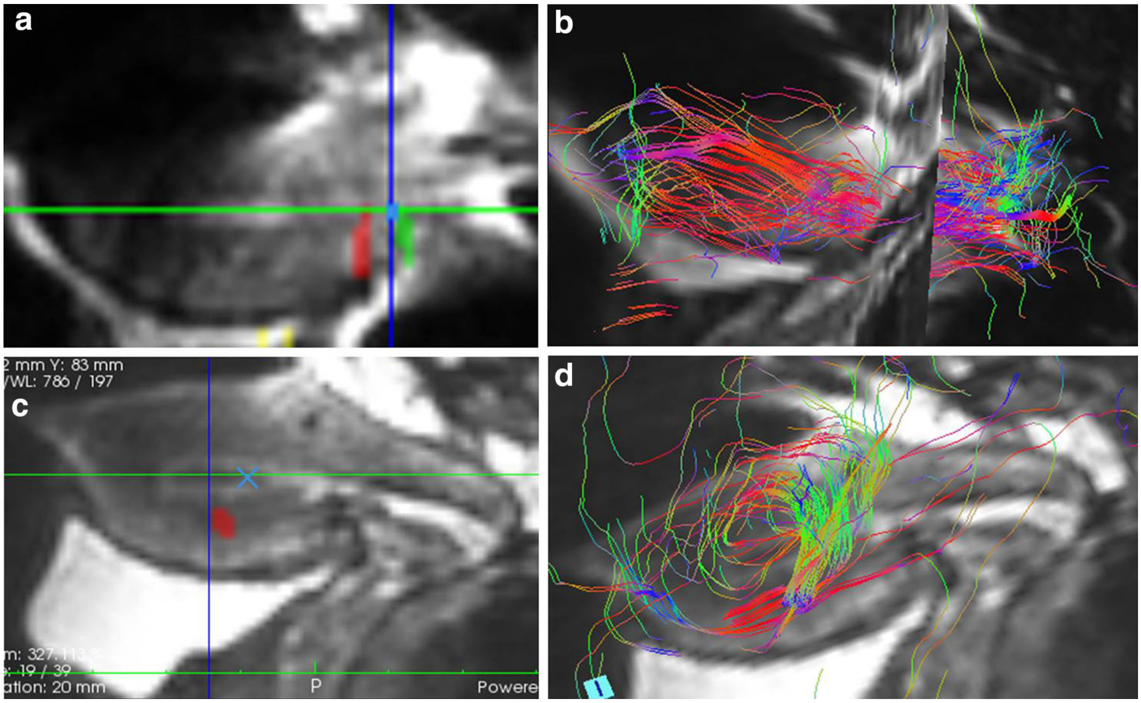

Fig. 3 Longitudinal and circular fibrers running between the regions of interest (ROIs) using 3T-MR with diffusion tensor imaging (DTI) with fiber tractography postprocessing software. **a** On para-sagittal SENSE-SSEPI at post-processing analysis, two similar ROIs were drawn at the anterior isthmus level. **b** 3T-MR-DTI with tractography reconstruction shows longitudinal bundles of fibres running through selected ROIs. **c** On para-sagittal SENSE-SSEPI at post-processing analysis, a single ROI was drawn in the inner myometrial layer. **d** 3T-MR-DTI with tractography reconstruction shows circular bundles of fibres running through selected ROI

group comparisons were performed using the two-tailed *t* test. All statistical analyses were conducted using Excel (Microsoft). The Spearman correlation test was used for the analysis of the association between the time elapsed since the CS and the percentage reduction in myometrial fibres running through the scar. Values are expressed as the mean ± SD or numbers with percentage in brackets or as the median with the IQ range.

Results

Forty-two women were enrolled in the study. Nineteen had one pCS (group 1), 11 had two pCS (group 2) and 12 women had one prior vaginal delivery. These latter received only 3T-MR examination and served as controls. Three subjects (group 1) were later excluded after both evaluations because of a retroflexed/retroverted uterus. One woman (group 1) was unable to continue the 3T-MR due to claustrophobia, and one woman (group 2) refused to undergo 3T-MR examination after receiving a TVUS evaluation. One woman (group 2) was also excluded after 3T-MR because of artefacts disturbing image acquisition due to an unreported tubal ligation during the second caesarean delivery. Therefore, a total of 36 women completed the study. The characteristics of the different groups are described in Table 1.

TVUS and 3T MR morphological comparison

As reported, uterine scars were subjectively classified as either "linear" or "retracting". According to 3T-MR, 12 cases were assessed as linear and 12 cases as retracting. According to TVUS, 20 cases were defined as linear and four cases as retracting. In 11 cases, there was agreement between the two imaging modalities (Figs. 4, 5). In 13 cases (54.1 %), 3T-MR and TVUS were discordant with 11 cases classified as retracting by 3T-MR and linear by TVUS (five were found in subjects with one pCS and six in those with two pCS) and with the opposite occurring in two cases (one in each group) (Figs. 6, 7).

Endometrial and myometrial thickness was measured on both T2 sequences (single-shot TSE and TSE) but no significant differences were found ($p > 0.5$), especially at the scar level. The reported measurements were made on SsTSE.

The average endometrial thickness was higher when measured with TVUS (7.5 ± 2.5 mm) compared to 3T-MR (6.14 ± 1.86 mm, $p = 0.002$).

Considering subjective description of the scar morphology with 3T-MRI, myometrium thickness at the scar

Table 1 Characteristics of the experimental groups

	Group I (19 women)	Group II (11 women)	Control group (12 women)
Age at first delivery	31.6 ± 2.3	33.0 ± 4.7	34 ± 2.7
Age at second delivery	N.A.	35.8 ± 5.8	N.A.
Months after last delivery	12.6 ± 6.9	13.6 ± 7.7	12.7 ± 6.5
Hysterorrhaphy at first delivery			N.A.
One layer of closure	10 (52.6 %)	6 (54.5 %)	
Two layers of closure	9 (47.4 %)	5 (45.5 %)	
Hysterorrhaphy at second delivery	N.A.		N.A.
One layer of closure		5 (45.5 %)	
Two layers of closure		6 (54.5 %)	
Birth weight at first delivery	3144 ± 512	3164 ± 544	3070 ± 450
Birth weight at second delivery	N.A.	3400 ± 338	N.A

The values are expressed as the mean ± SD or numbers with percentage in brackets. No statistically significant differences were found

N.A. not assessable

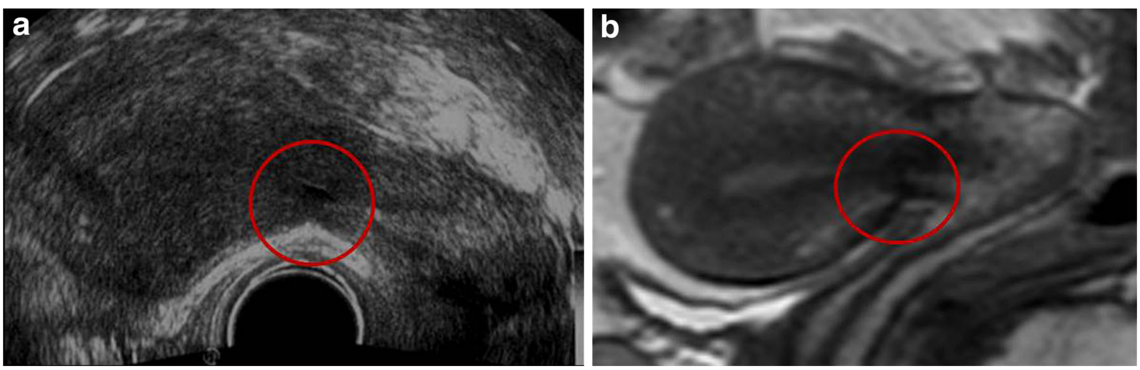

Fig. 4 40-year-old woman with one caesarean delivery. **a** TVUS image of caesarean scar classified as linear. **b** Para-sagittal T2 Ssh-TSE MR image of the same scar classified as linear

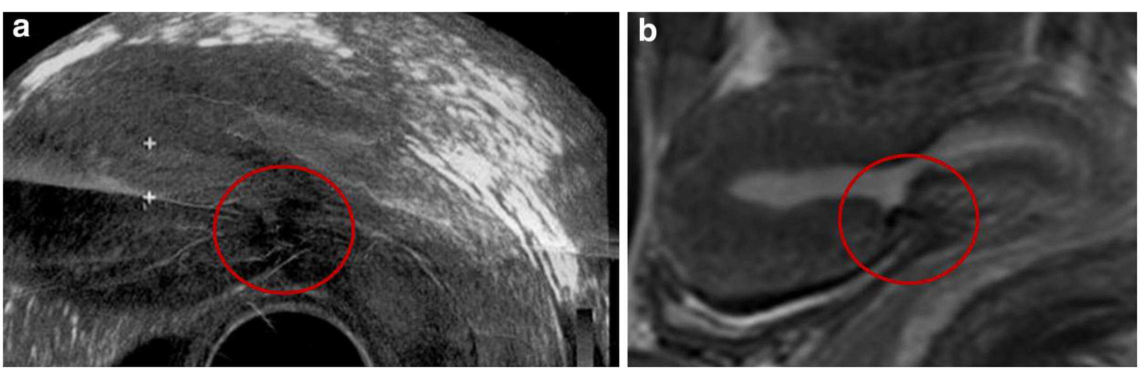

Fig. 5 33-year-old woman with double caesarean delivery. **a** TVUS image of caesarean scar classified as retracting. **b** Para-sagittal T2 Ssh-TSE MR image of the same scar classified as retracting

level was shown to be significantly higher (7.81 ± 1.40 mm, $p = 0.01$) compared to TVUS (5.83 ± 1.75 mm) among patients with a linear scar (Table 2). In patients with a retracting scar, there was no significant difference (Table 3).

Independent from scar morphology, the thickness of the myometrium upstream of the scar was measured as significantly greater by 3T-MR compared to TVUS (retracting 13.42 ± 2.8 vs. 9.6 ± 3.17 mm; $p = 0.011$ and linear 12.68 ± 2.24 vs. 8.50 ± 1.83 mm; $p = 0.0003$). Myometrium

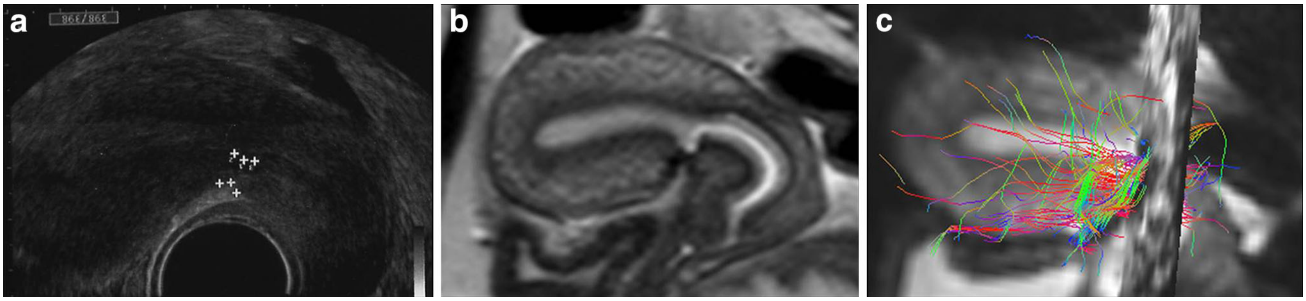

Fig. 6 32-year-old woman with single caesarean delivery. **a** TVUS image of caesarean scar classified as linear. **b** Para-sagittal T2 Ssh-TSE MR image of the same scar classified as retracting **c** 3T-MR-DTI SENSE-SSEPI image with tractography reconstruction shows longitudinal bundle of fibres running through the anterior isthmus (−67 % fibre reduction)

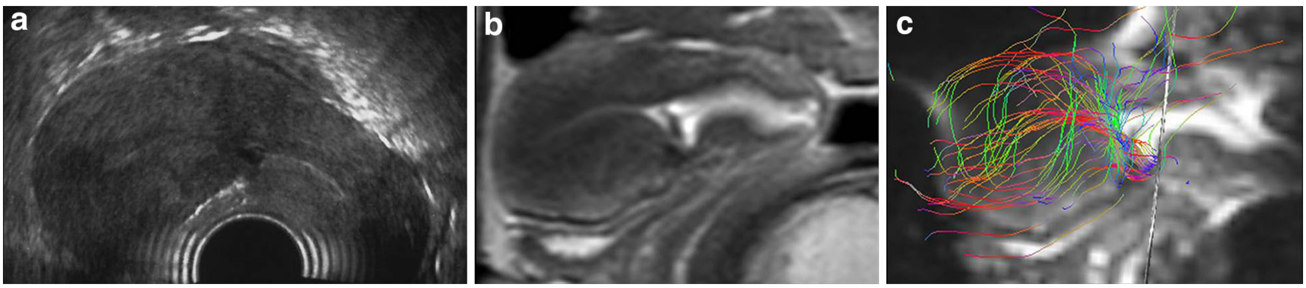

Fig. 7 39-year-old woman with double caesarean delivery **a** TVUS image of caesarean scar classified as linear. **b** Para-sagittal T2 Ssh-TSE MR image of the same scar classified as retracting **c** 3T-MR-DTI SENSE-SSEPI image with tractography reconstruction shows longitudinal bundle of fibres running through the anterior isthmus (−52 % fibre reduction)

Table 2 Thickness of the endometrium and myometrium at different levels measured with 3-Tesla magnetic resonance (3T-MR) imaging and transvaginal ultrasound (TVUS) in women with "linear" scar morphology

Level	3T MR (mm)	TVUS (mm)	*p* value (*t* test)
Endometrium	5.86 ± 2.27	7.42 ± 3.23	0.02
Myometrium scar	7.81 ± 1.40	5.83 ± 1.75	0.01
Myometrium upstream of the scar	12.68 ± 2.24	8.50 ± 1.83	<0.001
Myometrium downstream of the scar	9.46 ± 1.59	7.67 ± 1.87	0.03

The values are expressed as the mean ± SD

Table 3 Thickness of the endometrium and myometrium at different levels measured-Tesla magnetic resonance (3T-MR) imaging and transvaginal ultrasound (TVUS) in women with "retracting" scar morphology

Level	3T MR (mm)	TVUS (mm)	*p* value (*t* test)
Endometrium	6.42 ± 1.38	7.50 ± 1.62	0.05
Myometrium scar	5.5 ± 1.51	6.71 ± 3.11	NS
Myometrium upstream of the scar	13.42 ± 2.81	9.63 ± 3.17	0.01
Myometrium downstream of the scar	9.75 ± 2.14	9.83 ± 4.3	NS

The values are expressed as the mean ± SD

thickness downstream of the linear scar was higher when measured with 3T-MRI compared to TVUS ($p = 0.033$). However, in subjects with retracting scar morphology, there was no significant difference in the myometrium thickness downstream of the scar.

Measurement of fibre density

MR-DTI image reconstruction was possible in every case. In the control group, the expected uterine muscular structure was well shown and highlighted the extremely structured muscular tissues of the inner circular and external longitudinal layers (Fig. 7). The mean MR-DTI processing time was 90 ± 19 min, with a significantly longer time for the pCS groups (120 ± 18 min) compared to the control group (60 ± 20 min) due to the altered uterine structure.

In patients with a single pCS, MR-DTI with 3D tractography reconstruction analysis showed a reduction in the percentage of longitudinal myometrial fibres running through the uterine scar in the anterior wall compared to the posterior wall at the same level (Fig. 8). Overall, patients with pCS showed a decrease in longitudinal myometrial fibres in the anterior versus posterior wall,

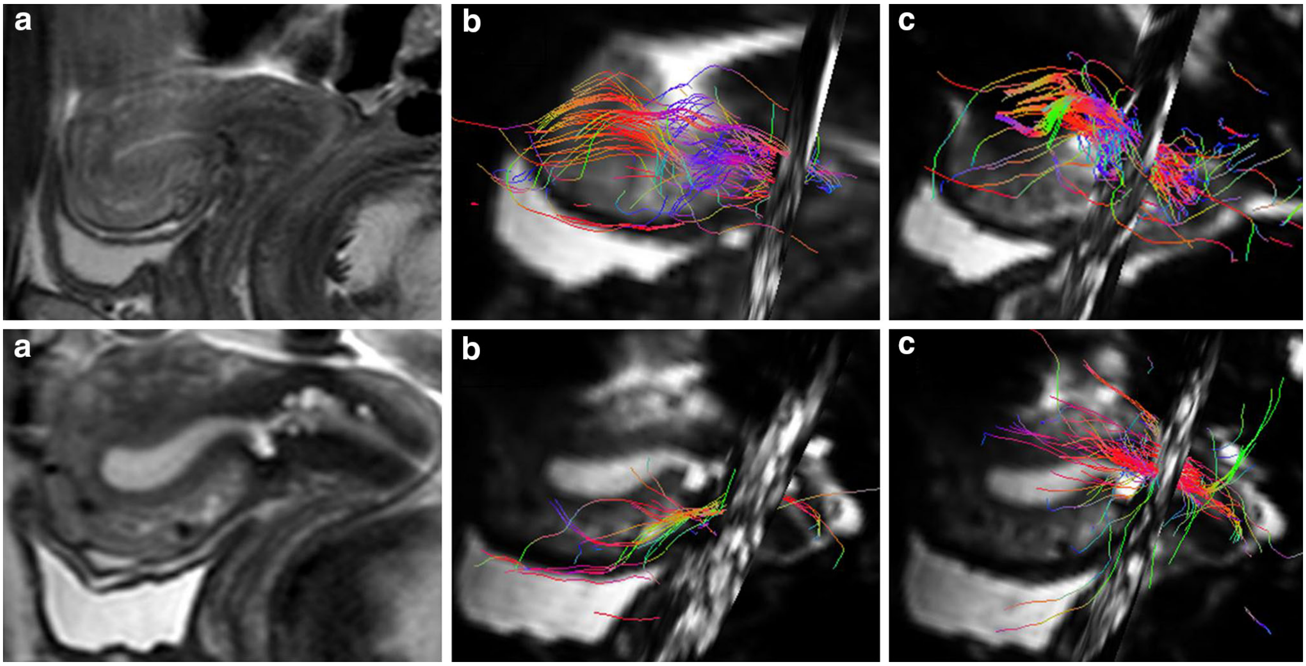

Fig. 8 Degree of disarray of fibres running through selected ROIs with 3T-RM-DTI with tractography reconstruction. Top row: 35-year-old woman with single caesarean delivery. **a** Para-sagittal TSE T2 image of linear caesarean scar without endometrial alteration. 3T-MR-DTI SENSE-SSEPI image with tractography reconstruction shows longitudinal bundle of fibres running through **b** anterior isthmus and **c** posterior wall at the same level showing a low degree of disarray (−30 % fibre reduction). Bottom row: 37-year-old woman with two caesarean deliveries. **a** Para-sagittal TSE T2 image of retracting caesarean scar with endometrial deihiscence. 3T-MR-DTI SENSE-SSEPI image with tractography reconstruction shows longitudinal bundle of fibres running through **b** anterior isthmus and **c** posterior wall at the same level showing a high degree of disarray (−90 % fibre reduction). Fibres outside the uterus can also be seen due to peristalsis artefacts

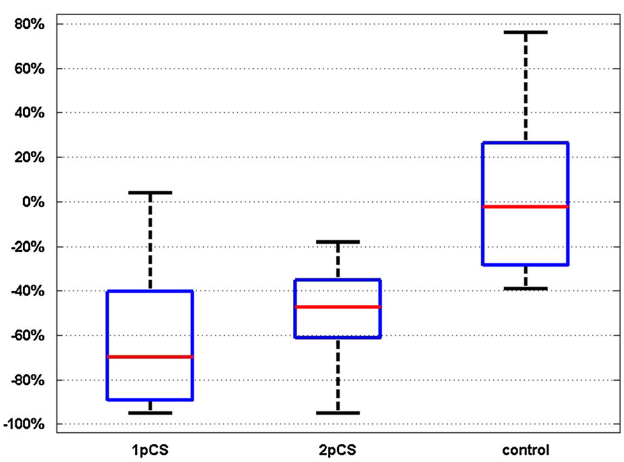

Fig. 9 Loss of isthmus scar fibre according to the number of previous caesarean section (pCS). *Red line* = median, *blue box* = interquartile range, *black dotted line* = range. Longitudinal myometrial fibres running in the anterior wall compared to the posterior wall, in comparison with the control group ($p < 0.001$). No statistically significant differences were found between groups 1 and 2

which was significantly wider compared to controls (median with interquartile range: −53 %; −77 %, −34 % vs. −2 %; −27 %, 22 %, $p < 0.0001$). However, the median fibre reduction was not different in women with one pCS (−55 %; −79 %, −36 %) or two pCS (−46 %; −61 %, −35 %), $p = 0.47$ (Fig. 9).

In analysing the fibre reduction on the basis of scar morphology as detected by 3T-MRI, among women with a linear scar, the percentage of fibre reduction was significantly higher compared to the control group ($p < 0.001$) and the reduction was even more evident among women with a retracting scar compared to the control group ($p < 0.0001$). In addition, in retracting scars there was a significant fibre reduction (−65 %; IQ −45 %, −89 %) compared to linear scars (−46 %; IQ −14 %, −58 %; $p < 0.016$), underlining and confirming the higher grade of disruption of uterine muscular structure when the scar morphology appears to be highly altered.

As there was no difference in the reduction of fibre density in the scar between groups 1 and 2 (Fig. 9), we pooled both the groups to evaluate the effect of the time elapsed between CS and fibre density. When using the Spearman correlation, no association was found between the time elapsed since the CS and the percentage reduction of myometrial fibre running through the scar (Fig. 10).

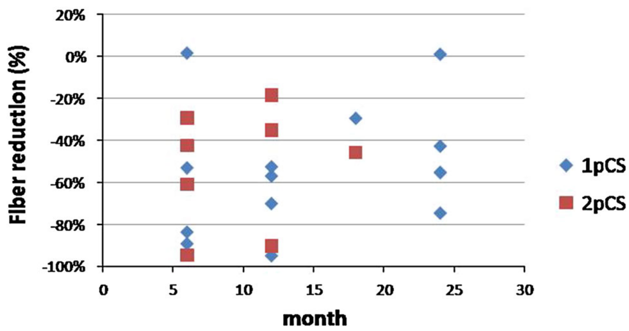

Fig. 10 Association between the time elapsed since the caesarean section (CS) and the percentage reduction in myometrial fibres running through the scar. No significant correlation was found

Discussion

Scar defects at the hysterotomy site in nonpregnant women have been shown to be common and described by many authors. Such scar defects have been found in 10–69 % of women who have undergone prior CS [23, 25]. The discrepancy of this finding might be explained by population differences or by measurement differences at TVUS techniques, although the measurements seem to have been taken in a similar manner as reported in the two studies [23, 25]. Our study shows a large discrepancy in the mapping of uterine scars between TVUS and 3T-MR and in terms of morphology; TVUS described 17 % of scars as retracting and 3T-MR 50 % of cases, confirming the large variability in scar description reported in the literature. Discordance in scar classification (as linear or retracted) was found in almost half of the cases, that is, 3T-MR and TVUS were concordant in 46 % and discordant in 54 % in morphological scar description. The different scar classification at 3T-MR and TVUS in our study could be explained by the higher contrast resolution of the 3T-MR technique, as well as the objective nature of MR evaluation compared with the more subjective nature of the TVUS examination. Surely the real-time imaging of TVUS favours the acquisition of sections that are orthogonal to the endometrial cavity, but also MRI with its intrinsic multiplanar acquisition potential can obtain proper uterine long and short axis, where morphological evaluation can be easily and accurately performed. Moreover, the obtained quantitative data from DTI reconstruction support the MR qualitative description. At 3T-MRI, measurements were made on both parasagittal fast Ssh-TSE T2 and TSE T2 sequences performed on the proper long axis of the uterus. No significant variations were found, especially when measuring scar thickness. The blurring artefact is well known in the literature [35, 36] but we used SENSE in image acquisition, which is known to reduce blurring artefacts due to the shortening of the echo-train length; moreover, the higher signal-to-noise ratio at 3 T helped in providing better image resolution despite the concomitant SNR increase. Echo-train SE has achieved widespread use, being insensitive to breathing artefacts whereas conventional T2 SE sequences are lengthy and suffer from patient motion and increased examination time. The major disadvantage of echo-train sequences is that T2 differences between tissues, especially at tissue-fat interface are decreased, but this is not relevant to our case since the endometrial–myometrial border was clearly identifiable. The interface at uterine level is not a tissue-fat interface but a muscle-glandular interface and we did not find any major or minor disturbing artefact. Motion due to the contracting bowel can cause image deterioration, and was responsible for the worst artefacts found in our study because no anti-peristaltic agent could be administered as per the study protocol. However, these artefacts did not influence scar measurement as they mostly affected the DTI reconstruction at the uterine fundus. Fast imaging, moreover, allowed for good resolution with shorter acquisition times and fewer peristaltic movement artefacts. Furthermore, bladder filling can cause major artefacts but only in DTI post-processing reconstruction since water protons of the urine can be mistaken by the software as belonging to water bound to myometrial fibres, lengthening the post-processing and re-processing times, so that the TSE sequence was performed as the last sequence of the study protocol. For all the above reasons, we decided to report the measurements taken on SsTSE and we suggest that 3T-MR could show a more accurate and reliable measurement both of myometrial thickness and scar morphology than TVUS. Obviously, the true thickness could only be obtained with direct tissue evaluation but that could not be performed in this population of women.

A significant difference between the two methods was found in the measurement of the myometrial thickness at the scar level. We suggest that 3T-MR could provide a more accurate and reliable measurement than TVUS, as the spatial resolution of the image is much higher. Upstream of the scar, TVUS measurements reported a significantly thinner myometrial layer compared to 3T-MR. Such underestimation could be one reason why screening for uterine scar defects or LUS thickness by TVUS is not very accurate at predicting future pregnancy complications [23, 24, 37–39]. For this reason, some authors suggest that TVUS evaluation of LUS should be combined with other information (previous single-layer closure of the uterus or inter-delivery interval) and such a multifactorial system seems to better predict the occurrence of uterine rupture during trial of labour [14]. Nowadays, none of the available noninvasive screening tools is sensitive enough to be clinically helpful in predicting an unsuccessful trial of labour in women with pCS and none has been validated prospectively to improve outcomes, as recently summarised by Berghella [39].

As described in our previous feasibility study [34], the MR-DTI microstructural analysis confirmed that the highly arranged uterine architecture is not preserved throughout the CS scar. Quantitative data obtained with 3D tractography reconstruction showed a varying degree of muscle fibre disruption within the scarred tissue and a reduction in the number of longitudinal fibres that run through the scar. Indeed, there was a significant decrease of longitudinal myometrial fibres in the scar tissue in subjects with pCS compared with primiparous women having had a vaginal delivery. Moreover, quantitative data obtained with 3T MR-DTI reconstruction supports the MR qualitative description of scar morphology. In those retracting scars undetected by TVUS, fibre density is significantly lower compared to linear scars. The clinical relevance of these data must be confirmed at follow-up, i.e. the mode of delivery of the volunteers in future pregnancies.

Unexpectedly, no difference in the extent of fibre reduction was found in women having had 1 vs 2 pCS. Again, there was no relationship between the number of pCS and the morphology of the scar tissue, with an equal distribution of linear and retracting morphology seen among the two groups. This is quite surprising, as previous studies with TVUS showed that multiple caesarean sections is a risk factor for larger scar defects [25, 40, 41] and that the rate of uterine rupture is higher in women with increasing numbers of pCS [13]. In any case, most obstetric guidelines advocate a trial of labour after pCS independently from the number of CS, and our quantitative data seem to support recent studies where also pregnant women with two pCS were admitted, if not contraindicated by other risk factors, to trial of labour [39].

One possible reason for this difference is the limited number of patients in our study, as well as the heterogeneity of time elapsed since pCS. Another explanation could originate from fibre tracking reconstruction software, as it is adapted from functional neurology, and it is possible that some of the disrupted muscular fibres could be erroneously quantified, which would lead to overestimation.

The evidence we found in the amount of fibre disruption induced by CS could support the current theory that associates abnormal placental insertions in the subsequent pregnancy of a scarred uterus [11, 40, 41]. Anecdotally, the subject with one pCS who went on to develop placenta previa in our series had the highest percentage reduction of longitudinal myometrial fibres (−95 %) within the retracting scar of the anterior isthmus region.

In conclusion, the results of our study challenge the idea that TVUS could be the gold standard for the assessment of LUS or scar defects in women with pCS. 3T-MR-DTI provides higher contrast image of the uterine scar morphology and appears to largely contradict the TVUS findings, which seem to underestimate myometrial thickness. The added values of 3T-MR with DTI and fibre tracking lie in the prompt evaluation of muscle remaining in the scars. The clinical application of such information remains to be assessed, as there are no literature reports addressing it. Nonetheless, the quantitative data of 3T-MR-DTI added to morphological evaluation could help the gynaecologist predict later complications of CS, and the identification of less disrupting scars could help in choosing vaginal birth after caesarean section.

Conflict of interest F. Fiocchi, E. Petrella, L. Nocetti, S. Currà, G. Ligabue, T. Costi, P. Torricelli, F. Facchinetti declare that none of the authors has a potential conflict of interest.

References

1. Martin JA, Hamilton BE, Ventura SJ et al (2011) Births: final data for 2009. Natl Vital Stat Rep 60:1–70
2. Getahun D, Oyelese Y, Salihu HM, Ananth CV (2006) Previous cesarean delivery and risks of placenta previa and placental abruption. Obstet Gynecol 107:771–778
3. Rasmussen S, Albrechtsen S, Dalaker K (2000) Obstetric history and the risk of placenta previa. Acta Obstet Gynecol Scand 79:502–507
4. Kastner ES, Figueroa R, Garry D, Maulik D (2002) Emergency peripartum hysterectomy: experience at a community teaching hospital. Obstet Gynecol 99:971–975
5. Fleisch MC, Lux J, Schoppe M et al (2008) Placenta percreta leading to spontaneous complete uterine rupture in the second trimester. Example of a fatal complication of abnormal placentation following uterine scarring. Gynecol Obstet Invest 65:81–83
6. Ben Nagi J, Ofili-Yebovi D, Marsh M, Jurkovic D (2005) First-trimester cesarean scar pregnancy evolving into placenta previa/accreta at term. J Ultrasound Med 24:1569–1573
7. Diaz SD, Jones JE, Seryakov M, Mann WJ (2002) Uterine rupture and dehiscence: ten-year review and case-control study. South Med J 95:431–435
8. Gilliam M (2006) Cesarean delivery on request: reproductive consequences. Semin Perinatol 30:257–260
9. Kennare R, Tucker G, Heard A, Chan A (2007) Risks of adverse outcomes in the next birth after a first cesarean delivery. Obstet Gynecol 109(2 Pt 1):270–276
10. Guise JM, McDonagh MS, Osterweil P et al (2004) Systematic review of the incidence and consequences of uterine rupture in women with previous caesarean section. Br Med J 329:19–25
11. Souza JP, Gülmezoglu A, Lumbiganon P et al (2010) WHO Global Survey on Maternal and Perinatal Health Research Group. Caesarean section without medical indications is associated with an increased risk of adverse short-term maternal outcomes: the 2004-2008 WHO Global Survey on Maternal and Perinatal Health. BMC Med 10:71
12. American College of Obstetricians and Gynecologists (2010) ACOG Practice bulletin no. 115: (2010) vaginal birth after previous cesarean delivery. Obstet Gynecol 116:450–463
13. Gholitabar M, Ullman R, James D, Griffiths M (2011) Guideline Development Group of the National Institute for Health and Clinical Excellence. Caesarean section: summary of updated NICE guidance. Br Med J 343:d7108

14. Bujold E, Jastrow N, Simoneau J et al (2009) Prediction of complete uterine rupture by sonographic evaluation of the lower uterine segment. Am J Obstet Gynecol 201(3):320.e1–320.e6
15. Fukuda M, Fukud K, Mochizuki M (1988) Examination of previous caesarean section scars by ultrasound. Arch Gynecol Obstet 243:221–224
16. Rozenberg P, Goffinet P, Phillippe HG, Nisand I (1996) Ultrasonographic measurement of lower uterine segment to assess risk of defects of scarred uterus. Lancet 347:281–284
17. Cheung VY, Constantinescu OC, Ahluwalia BS (2004) Sonographic evaluation of the lower uterine segment in patients with previous cesarean delivery. J Ultrasound Med 23:1441–1447
18. Cheung VY (2005) Sonographic measurement of the lower uterine segment thickness in women with previous caesarean section. J Obstet Gynaecol Can 27:674–681
19. Sen S, Malik S, Salhan S (2004) Ultrasonographic evaluation of lower uterine segment thickness in patients of previous cesarean section. Int J Gynaecol Obstet 87:215–219
20. Gotoh H, Masuzaki H, Yoshida A et al (2000) Predicting incomplete uterine rupture with vaginal sonography during the late second trimester in women with prior cesarean. Obstet Gynecol 95:596–600
21. Vikhareva Osser O, Valentin L (2010) Risk factors for incomplete healing of the uterine incision after caesarean section. Br J Obstet Gynaecol 117:1119–1126
22. Regnard C, Nosbusch M, Fellemans C et al (2004) Cesarean section scar evaluation by saline contrast sonohysterography. Ultrasound Obstet Gynecol 23:289–292
23. Ofili-Yebovi D, Ben-Nagi J, Sawyer E et al (2008) Deficient lower-segment Cesarean section scars: prevalence and risk factors. Ultrasound Obstet Gynecol 31:72–77
24. Armstrong V, Hansen WF, Van Voorhis BJ, Syrop CH (2003) Detection of cesarean scars by transvaginal ultrasound. Obstet Gynecol 101:61–65
25. Osser OV, Jokubkiene L, Valentin L (2009) High prevalence of defects in Cesarean section scars at transvaginal ultrasound examination. Ultrasound Obstet Gynecol 34:90–97
26. Osser OV, Jokubkiene L, Valentin L (2010) Cesarean section scar defects: agreement between transvaginal sonographic findings with and without saline contrast enhancement. Ultrasound Obstet Gynecol 35:75–83
27. Lim RP, Lee VS, Bennett GL et al (2006) Imaging the female pelvis at 3.0 T. Top Magn Reson Imaging 17:427–443
28. Beddy P, O'Neill AC, Yamamoto AK et al (2012) FIGO staging system for endometrial cancer: added benefits of MR imaging. Radiographics 32:241–254
29. Langer JE, Oliver ER, Lev-Toaff AS, Coleman BG (2012) Imaging of the female pelvis through the life cycle. Radiographics 32:1575–1597
30. Rodgers SK, Kirby CL, Smith RJ, Horrow MM (2012) Imaging after cesarean delivery: acute and chronic complications. Radiographics 32:1693–1712
31. Palacios Jaraquemada JM, Bruno CH (2005) Magnetic resonance imaging in 300 cases of placenta accreta: surgical correlation of new findings. Acta Obstet Gynecol Scand 84:716–724
32. Mukherjee P, Berman JI, Chung SW et al (2008) Diffusion tensor MR imaging and fibre tractography: theoretic underpinnings. Am J Neuroradiol 29:632–664
33. Weiss S, Jaermann T, Schmid P et al (2006) Three-dimensional fibre architecture of the nonpregnant human uterus determined ex vivo using magnetic resonance diffusion tensor imaging. Anat Rec A Discov Mol Cell Evol Biol 288:84–90
34. Fiocchi F, Nocetti L, Siopis E et al (2012) In-vivo 3T magnetic resonance diffusion tensor imaging for detection of the fibre architecture of the human uterus: a feasibility and quantitative study. Br J Radiol 85:e1009–e1017
35. Li T, Mirowitz SA (2003) Fast T2-weighted MR imaging: impact of variation in pulse sequence parameters on image quality and artifacts. Magn Reson Imaging 21:745–753
36. Martin DR, Friel HT, Danrad R et al (2005) Approach to abdominal imaging at 1.5 Tesla and optimization at 3 Tesla. Magn Reson Imaging Clin N Am 13:241–254
37. Rozenberg P, Goffinet F, Phillippe HJ, Nisand I (1996) Ultrasonographic measurement of lower uterine segment to assess risk of defects of scarred uterus. Lancet 347:281–284
38. Tanik A, Ustun C, Cil E, Arslan A (1996) Sonographic evaluation of the wall thickness of the lower uterine segment in patients with previous cesarean section. J Clin Ultrasound 24:355–357
39. Berghella V (2012) Maternal-Fetal & Obstetric Evidence Based Guidelines, two-volume set, 2nd edn. (ISBN-10:1841848263; ISBN-13: 978-1841848266)
40. Wang CB, Chiu WWC, Lee CY et al (2009) Cesarean scar defect: correlation between Cesarean section number, defect size, clinical symptoms and uterine position. Ultrasound Obstet Gynecol 34:85–89
41. Usta IM, Hobeika EM, Musa AA et al (2005) Placenta previa-accreta: risk factors and complications. Am J Obstet Gynecol 193:1045–1049